EAN 2014
52nd conference on experimental stress analysis

Progressive Failure Analysis of Sandwich Beam in Case of Transversely Low-Velocity Impact

MANDYS Tomáš[1,a], LAŠ Vladislav[1,b], KROUPA Tomáš[2,c] and ZEMČÍK Robert[2,d]

[1]University of West Bohemia in Pilsen, NTIS - New Technologies for information Society, Univerzitní 22, 306 14 Plzeň, Czech Republic

[2]University of West Bohemia in Pilsen, Faculty of Applied Sciences, Department of Mechanics, Univerzitní 22, 306 14 Plzeň, Czech Republic

[a]tmandys@ntis.zcu.cz, [b]las@kme.zcu.cz, [c]kroupa@kme.zcu.cz, [d]zemcik@kme.zcu.cz

Keywords: Sandwich composite panel, fiber-glass fabric, foam core, low-velocity impact, damage.

Abstract. This contribution is focused on the progressive failure analysis of sandwich composite beam loaded with transversely low-velocity impact. A user defined material model was used for modeling of the non-linear orthotropic elastic behavior of composite skin. The non-linear behavior of foam core was modeled using Low-Density Foam material model. The numerical model was validated using performed experiment and the results in terms of deflection and contact force time dependencies are mutually compared.

Introduction

The sandwich structures are based on the principle of low density material (core) placed between two stiffer and thinner outer skins. The main purpose of the core is to maintain the distance between outer skins ant to transfer the shear load while the outer skin carry the compressive and tensile loads. The sandwich structures are widely used in many kind of structural applications where the weight must be kept to a minimum value [1]. It is due to their high stiffness an strength to weight ratios in comparison to conventional materials, environmental resistance and product variability. The main disadvantage of sandwich structures is their predisposition to damage and failure caused in case of low-velocity impacts with foreign objects [2]. The damage of sandwich structures can be detected using CT-scan [2] or using structural health monitoring (SHM) [3].

This work deals with the experimental investigation and numerical modeling of behavior of wide composite sandwich beam subjected to transversely low-velocity impact. The tested composite sandwich panel of overall thickness 12.5 mm was manufactured using vacuum infusion process. The outer laminated composite skins of thickness 1.2 mm were made from 3 layers of fiber-glass fabric Aeroglass and epoxy resin Epicote HGS LR 285. The core of the sandwich was a closed cell cross-linked polymer foam Airex C70.55 that is characterized by low resin absorption. Resultant sandwich panel was cured for 6 hours at temperature 50 °C.

Material Model of Composite Skin

A user defined material model of composite skin considering the non-linear elastic behavior was implemented using VUMAT subroutine written in Fortran code. The non-linear function describing the stress-strain relationship starting from deformation ε_{0i} (i = 1, 2) is assumed in case of principal material directions 1 and 2 (Eq. 2 and Eq. 4). The non-linear function with constant asymptote (Eq. 6) is considered in case of plane shear in principal directions 1 and 2 [4]. The following equations describe the resulting stress strain relationship of composite skin

$$\sigma_1 = C_{11}\cdot\varepsilon_1 + C_{12}\cdot\varepsilon_2 + C_{13}\cdot\varepsilon_3, \text{ for } \varepsilon_1 < \varepsilon_{01}, \tag{1}$$

$$\sigma_1 = \left(C_{11}\cdot\left[\varepsilon_1 + \frac{A_1}{2}\cdot\left(\varepsilon_{01}^2 - \varepsilon_1^{\,2}\right) - A_1\cdot\varepsilon_{01}\cdot\left(\varepsilon_{01} - \varepsilon_1\right)\right] + C_{12}\cdot\varepsilon_2 + C_{13}\cdot\varepsilon_3\right)\cdot\left(1-D\right), \text{ for } \varepsilon_1 \geq \varepsilon_{01}, \tag{2}$$

$$\sigma_2 = C_{12}\cdot\varepsilon_1 + C_{22}\cdot\varepsilon_2 + C_{23}\cdot\varepsilon_3, \text{ for } \varepsilon_2 < \varepsilon_{02}, \tag{3}$$

$$\sigma_2 = \left(C_{12}\cdot\varepsilon_1 + C_{22}\cdot\left[\varepsilon_2 + \frac{A_2}{2}\cdot\left(\varepsilon_{02}^2 - \varepsilon_2^{\,2}\right) - A_2\cdot\varepsilon_{02}\cdot\left(\varepsilon_{02} - \varepsilon_2\right)\right] + C_{23}\cdot\varepsilon_3\right)\cdot\left(1-D\right), \text{ for } \varepsilon_2 \geq \varepsilon_{02}, \tag{4}$$

$$\sigma_3 = \left(C_{13}\cdot\varepsilon_1 + C_{23}\cdot\varepsilon_2 + C_{33}\cdot\varepsilon_3\right)\cdot\left(1-D\right), \tag{5}$$

$$\tau_{12} = \frac{G_{12}^0\cdot\gamma_{12}}{\left[1+\left(\frac{G_{12}^0\cdot\left|\gamma_{12}\right|}{\tau_{12}^0}\right)^{n_{12}}\right]^{\left(\frac{1}{n_{12}}\right)}}\cdot\left(1-D\right), \tag{6}$$

$$\tau_{23} = \left(G_{23}\cdot\gamma_{23}\right)\cdot\left(1-D\right), \tag{7}$$

$$\tau_{13} = \left(G_{13}\cdot\gamma_{13}\right)\cdot\left(1-D\right), \tag{8}$$

where

$$C_{11} = \frac{E_1\cdot\left[1-\nu_{23}\cdot\nu_{32}\right]}{\Delta}, \quad C_{12} = \frac{E_1\cdot\left[\nu_{21}+\nu_{23}\cdot\nu_{32}\right]}{\Delta}, \quad C_{13} = \frac{E_1\cdot\left[\nu_{31}+\nu_{32}\cdot\nu_{21}\right]}{\Delta},$$

$$C_{22} = \frac{E_2\cdot\left[1-\nu_{31}\cdot\nu_{13}\right]}{\Delta}, \quad C_{23} = \frac{E_2\cdot\left[\nu_{32}+\nu_{31}\cdot\nu_{12}\right]}{\Delta}, \quad C_{33} = \frac{E_3\cdot\left[1-\nu_{12}\cdot\nu_{21}\right]}{\Delta}, \tag{9}$$

$$\Delta = 1-\nu_{12}\cdot\nu_{21}-\nu_{23}\cdot\nu_{32}-2\cdot\nu_{12}\cdot\nu_{23}\cdot\nu_{31}.$$

The material parameters E_1, E_2 and E_3 are Young's moduli in principal directions 1, 2 and 3; and ν_{12}, ν_{23}, ν_{31} Poisson's ratios in planes defined by principal directions 1, 2 and 3. Shear modulus in plane 2 3 and 1 3, is designated as G_{23} and G_{13}, respectively. The parameters A_1 and A_2 describe the straightening of yarns of fiber-glass fabric and the loss of stiffness in corresponding directions 1 and 2. The values of deformations ε_{01} and ε_{02} indicate the transitions between linear and non-linear parts of stress-strain relationship in the principal directions 1 and 2 during the loading. The nonlinear behavior in case of shear in plane 1 2 (Eq. 6) is described using initial shear modulus G_{12}^0, asymptotic value of shear stress τ_{12}^0 and shape parameter n_{12}.

The maximum stress failure criterion was used for prediction of failure of composite skin in form

$$F_{1T} = \frac{\sigma_1}{X_T}, \quad F_{1C} = \frac{\left|\sigma_1\right|}{X_C}, \quad F_{2T} = \frac{\sigma_2}{Y_T}, \quad F_{2C} = \frac{\left|\sigma_2\right|}{Y_C}, \quad F_{12} = \frac{\tau_{12}}{S_L}, \tag{10}$$

where X and Y are the strengths in principal directions 1 and 2, the subscripts T and C denote tension and compression and S_L is the shear strength. The values of degradation variable D are dependent on the type of occurred failure [5]. The degradation parameter in case of shear failure ($F_{12} \geq 1.0$ and $\gamma_{12} \geq \gamma_{12}^F$) was implemented from [6]. The degradation parameters are presented in different kinds of occurring failure in forms

$$\begin{aligned} &F_{1T} \geq 1 \Rightarrow D = 1.0, \quad F_{2T} \geq 1 \Rightarrow D = 1.0, \quad F_{12} \geq 1 \text{ and } \gamma_{12} \leq \gamma_{12}^F \Rightarrow D = 1 - e^{\left(\frac{1}{m_{12}} \cdot (F_{12})^{m_{12}}\right)}, \\ &F_{1C} \geq 1 \Rightarrow D = 0.6, \quad F_{2C} \geq 1 \Rightarrow D = 0.6, \quad F_{12} \geq 1 \text{ and } \gamma_{12} > \gamma_{12}^F \Rightarrow D = 1.0, \end{aligned} \tag{11}$$

where the non-negative constant m_{12} is presented by integer and γ_{12}^F is the ultimate deformation when the material is fully damaged. The principle of linear and non-linear material behavior together with the principle of degradation is shown in Fig. 1. The principle of non-linear function with constant asymptote and applied material degradation is presented Fig. 2. The material parameters were identified from tensile and compressive tests of composite skin using mathematical optimization process. Parameters E_3, G_{23} and G_{13} were taken from [7]. All material parameters are summarized in Table 1.

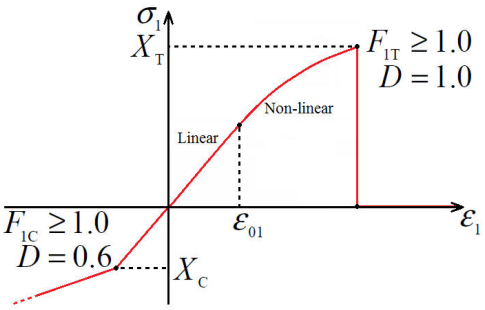

Fig. 1. The principle of linear and non-linear material behavior together with material degradation in principal direction 1.

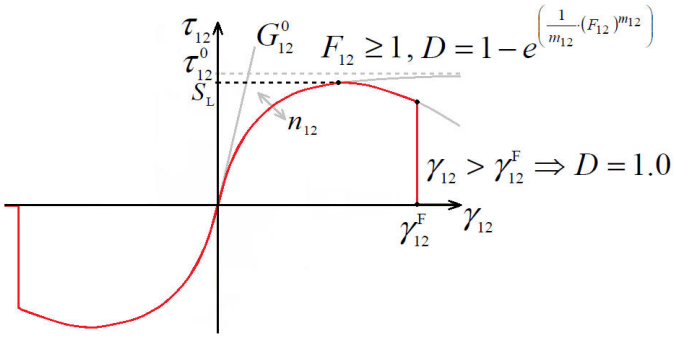

Fig. 2. The principle of material degradation of non-linear function with constant asymptote in plane 1 2.

Table 1. Material parameters of composite skin.

E_1 [GPa]	E_2 [GPa]	E_3 [GPa]	G_{13} [GPa]	G_{23} [GPa]	A_1 [–]	A_2 [–]	ε_{01} [–]	ε_{02} [–]	τ_{12}^0 [MPa]	m_{12} [–]
16.9	18.5	8.0	4.0	2.75	10.0	14.0	0.0008	0.005	39.66	5
ν_{12} [–]	ν_{23} [–]	ν_{31} [–]	γ_{12}^F [–]	G_{12}^0 [GPa]	X_T [MPa]	X_C [MPa]	Y_T [MPa]	Y_C [MPa]	S_L [MPa]	ρ_C [kg·m^{-3}]
0.337	0.337	0.28	0.32	4.96	325	65	347	67	35	1154

Material Model of Foam Core

The Low-Density Foam material model [8] intended for highly compressible elastomeric foams was used for modeling of foam core of sandwich structure. The isotropic material behavior that assumed the zero Poisson's ratio was specified directly via unaxial stress-strain curves for tension and compression. The Fig. 3 shows the considered compressive and tensile

stress-strain relationship of foam core. The tension stress-strain behavior was described via curve in form

$$\sigma(\varepsilon) = 92.6 \cdot \ln(1+\varepsilon) + 198.8 \cdot [\ln(1+\varepsilon)]^2 - 134.2 \cdot [\ln(1+\varepsilon)]^3 - 2.3 \cdot [\ln(1+\varepsilon)]^4 + 11.8 \cdot [\ln(1+\varepsilon)]^5. \quad (12)$$

The material is fully damaged after reaching tensile strength R_{mT}. The compressive stress-strain behavior was described as ideally elastoplastic material with Young's moduli E and yield limit R_{mC}. The all used material parameters are summarized in Table 2.

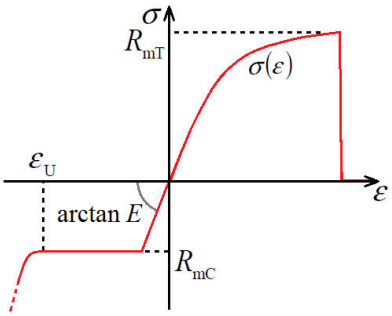

Fig. 3. Compressive and tensile stress-strain behavior of foam core.

Table 2. Material parameters of foam core.

E	ν	R_{mT}	R_{mC}	ε_U	ρ_f
[MPa]	[–]	[MPa]	[MPa]	[–]	[$kg \cdot m^{-3}$]
50.0	0.0	1.5	1.2	0.53	60

Experiment

The sandwich composite beam having the dimensions 490 mm × 50 mm and thickness 12.5 mm was subjected to transverse low-velocity impact using drop-testing machine. The testing device enables to set the starting height of impactor and the impact place on tested body directly via moveable vertical and horizontal linear guides. The impactor was equipped by force sensor (Brüel&Kjær 8200) that enables to record the time-force response (contact force) between the head of impactor and tested body. Spherical head of impactor had radius 15 mm. The impactor of total weight 2.211 kg was accelerated only by the gravity and the impacts were aimed at the center of upper skin of sandwich beams. The range of impact velocities was varied between $1.0\,m \cdot s^{-1}$ and $4.0\,m \cdot s^{-1}$, namely $1.0\,m \cdot s^{-1}$, $2.0\,m \cdot s^{-1}$, $2.25\,m \cdot s^{-1}$, $2.5\,m \cdot s^{-1}$, $3.0\,m \cdot s^{-1}$ and $4.0\,m \cdot s^{-1}$. The response of sandwich was measured in form of deflection in selected point (see Fig. 4) using the laser sensor (OptoNCDT 2200). The sampling frequency of force sensor and laser sensor was the same, 10 kHz. The sandwich beams were simply supported on the steel stand along the shorter edge. The distances of supports were 400 mm. The overall experimental apparatus with geometry is shown on Fig. 4. The impact events were recorded using high-speed digital camera (Olympus i-Speed 2) with 2000 fps. Fig. 5 shows the process of impact event from high-speed camera for impact velocity $4.0\,m \cdot s^{-1}$. The occurrence of damage of upper composite skin starting at time t = 0.0045 s is shown obvious from pictures.

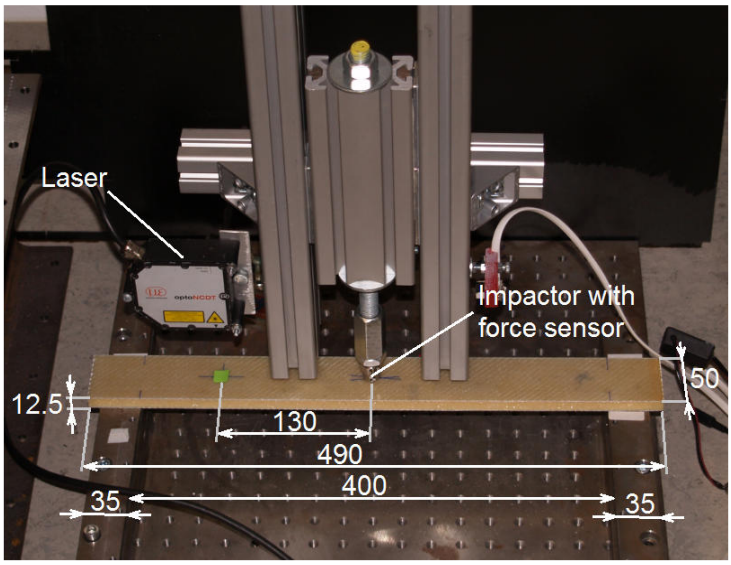

Fig. 4. Experimental apparatus with geometry of sandwich composite beam.

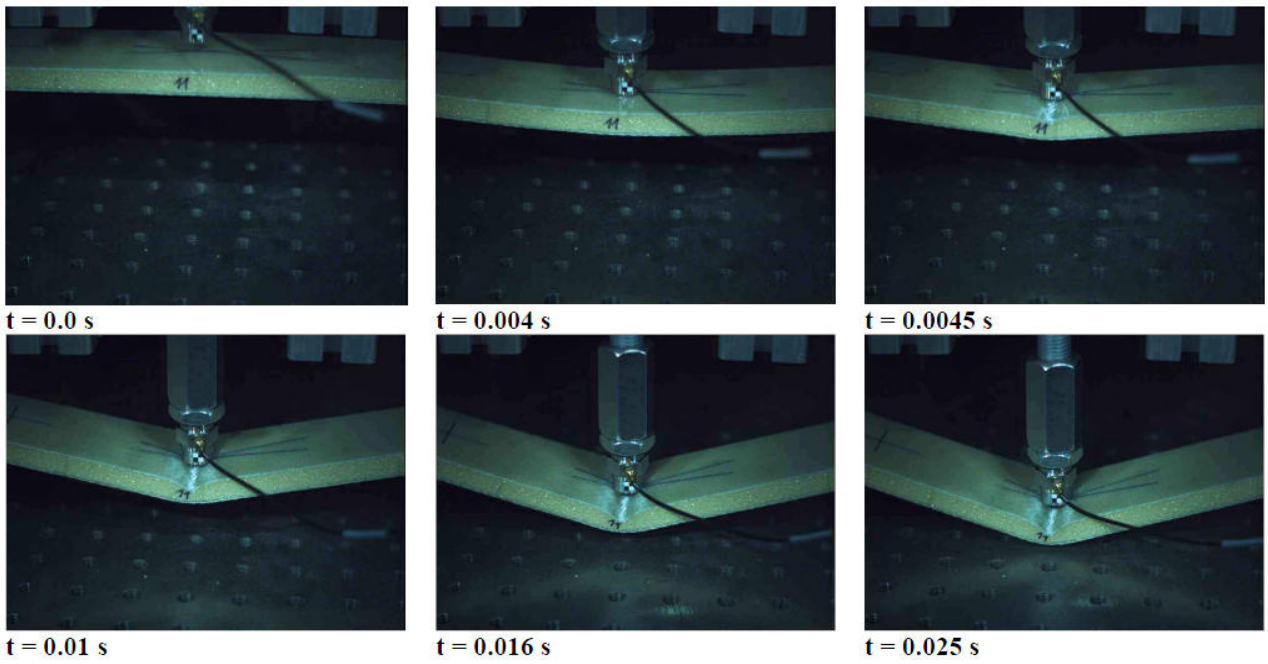

Fig. 5. Sequence of impact event from high-speed camera for impact velocity $4.0\,\mathrm{m}\cdot\mathrm{s}^{-1}$.

Numerical Simulations and Results

The numerical simulations were modeled in finite element method software Abaqus 6.11 using explicit solver based on central difference scheme for time integration. The finite strain theory was assumed. The finite element model was created as a full contact problem of four bodies. 8-node solid elements (Type C3D8R) were used. The friction between bodies has been neglected. The finite element model of impactor was simplified and only the head of impactor was modeled with added mass to reach its real total weight. The weight and stiffness of attached cable of force sensor placed in head of impactor was neglected. The comparison of deflections and contact forces dependencies on the time is shown for particular impact velocities on Figs. 6-11. The results are compared for the range t = 0 - 30 ms from the start of impact event. The occurrence of failure starts from impact velocity $2.5\,\mathrm{m}\cdot\mathrm{s}^{-1}$ in case on

experiments and $3.0\,\mathrm{m}\cdot\mathrm{s}^{-1}$ in case of numerical simulations. The upper composite skin was fractured under the impactor in each case.

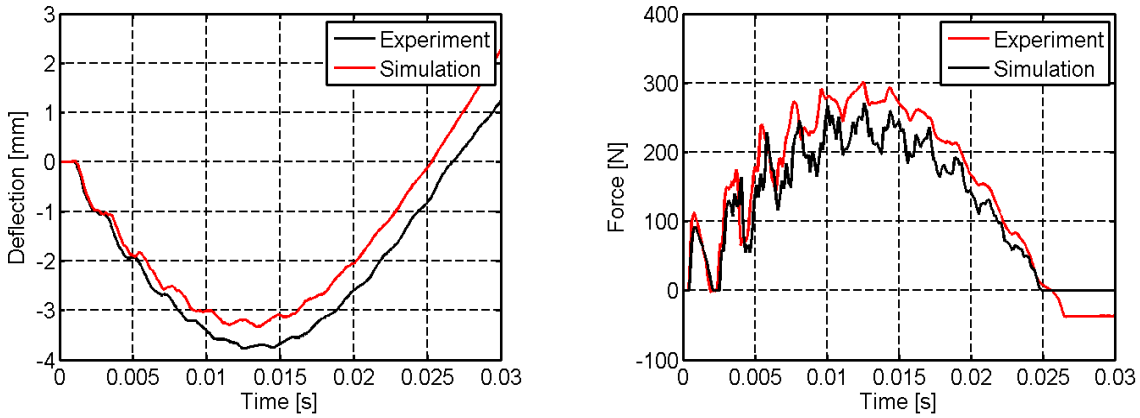

Fig. 6. Comparison of deflection (left) and contact force (right) between numerical simulation and experiment for impact velocity $1.0\,\mathrm{m}\cdot\mathrm{s}^{-1}$.

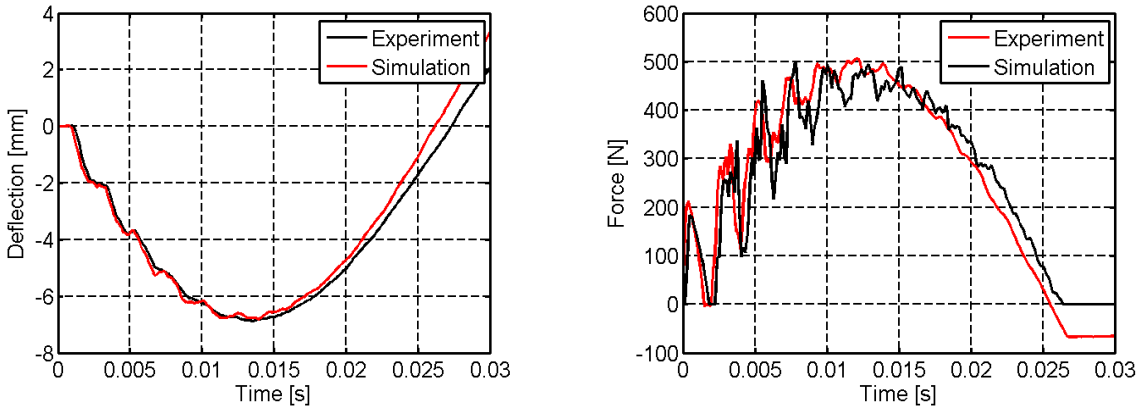

Fig. 7. Comparison of deflection (left) and contact force (right) between numerical simulation and experiment for impact velocity $2.0\,\mathrm{m}\cdot\mathrm{s}^{-1}$.

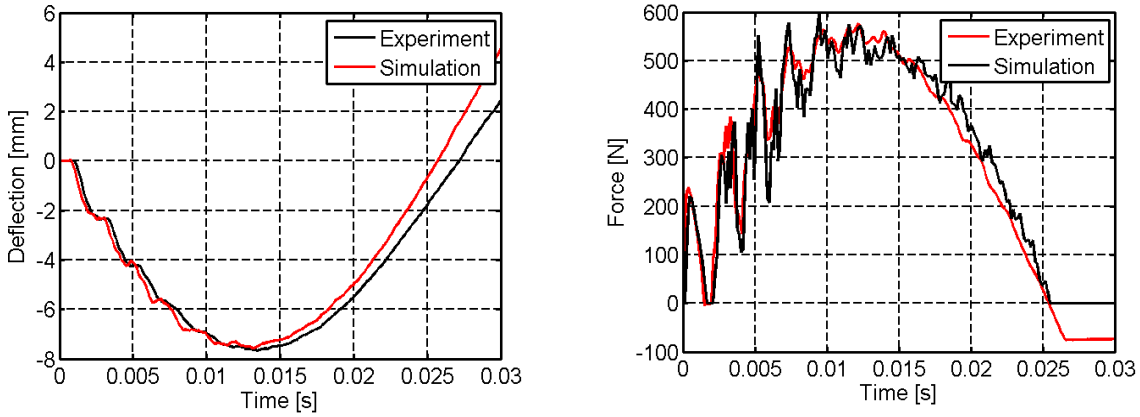

Fig. 8. Comparison of deflection (left) and contact force (right) between numerical simulation and experiment for impact velocity $2.25\,\mathrm{m}\cdot\mathrm{s}^{-1}$.

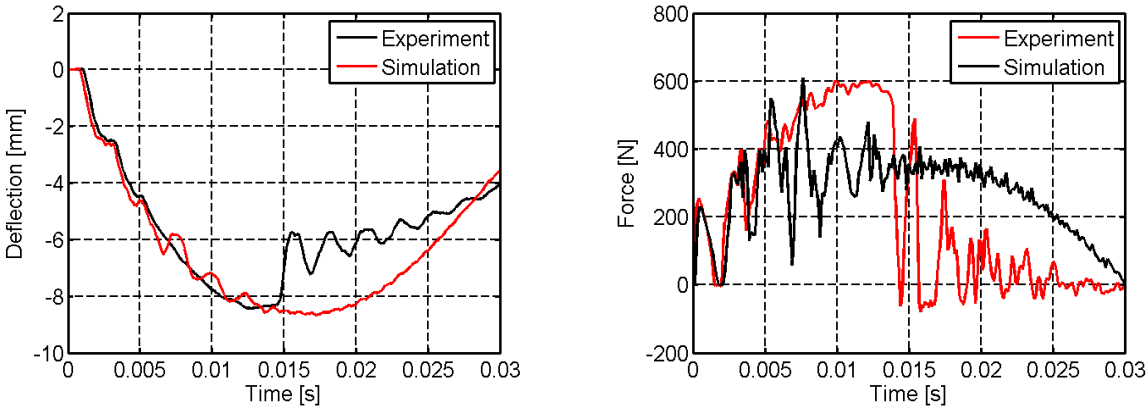

Fig. 9. Comparison of deflection (left) and contact force (right) between numerical simulation and experiment for impact velocity $2.5\ \mathrm{m \cdot s^{-1}}$.

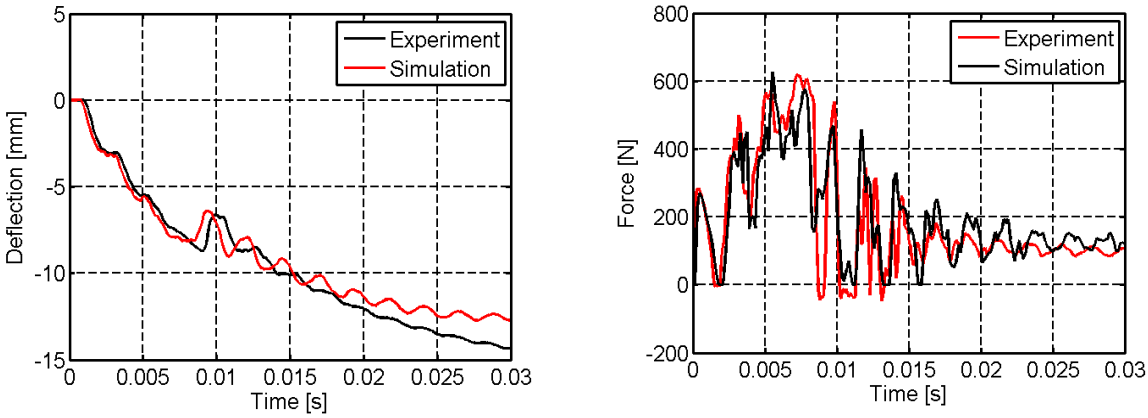

Fig. 10. Comparison of deflection (left) and contact force (right) between numerical simulation and experiment for impact velocity $3.0\ \mathrm{m \cdot s^{-1}}$.

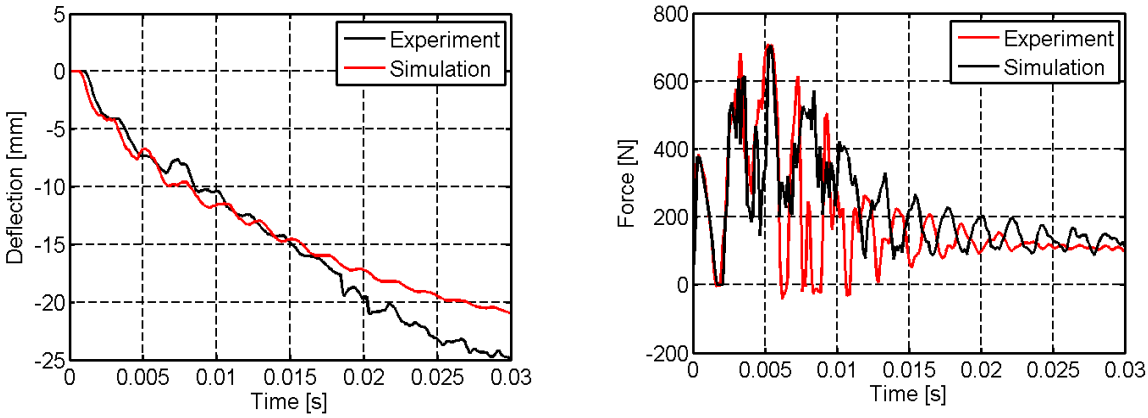

Fig. 11. Comparison of deflection (left) and contact force (right) between numerical simulation and experiment for impact velocity $4.0\ \mathrm{m \cdot s^{-1}}$.

Conclusions

The response of composite sandwich beam to low-velocity impact has been investigated experimentally and numerically. The experimental results in form of deflection and contact force time dependencies were compared with results from numerical model for all performed impact velocities. The failure of upper composite skin first occurred at impact velocity

$2.5\,\mathrm{m}\cdot\mathrm{s}^{-1}$ in case of experimental testing and at $3.0\,\mathrm{m}\cdot\mathrm{s}^{-1}$ in case of numerical simulation. The future work will be aimed on user defined material model describing the non-linear behavior of low-density foams.

Acknowledgement

The work has been supported by the European Regional Development Fund (ERDF), project "NTIS – New Technologies for Information Society", European Centre of Excellence, CZ.1.05/1.1.00/02.0090, the student research project of Ministry of Education of Czech Republic No. SGS-2013-036 and the project of Grant Agency of the Czech Republic No. GAČR P101/11/0288.

References

[1] M. Meo, A.J. Morris, R. Vignjevic, G. Marengo, Numerical simulations of low-velocity impact on an aircraft sandwich panel, Composite Structures 62 (2003) 353-360.

[2] J. Wang, A.M. Waas, H. Wang, Experimental and numerical study on the low-velocity impact behavior of foam-core sandwich panels, Composite Structures 96 (2013) 298-311.

[3] P. Sadílek, R. Zemčík, J. Bartošek, T. Mandys, Active structural health monitoring of composite plates and sandwiches, Applied and Computational Mechanics 7 (2013) 183-192.

[4] T. Kroupa, R. Zemčík, J. Klepáček, Temperature dependence of parameters of non-linear stress-strain relationship for carbon epoxy composites, Materiali and Technologije 43 (2009) 69-72.

[5] V. Laš, R. Zemčík, Progressive damage of undirectional composite panel. Journal of Composite Materials 42 (2008) 22-44.

[6] C.F. Yen, Ballistic Impact modeling of composite materials, in: 7th International LS-Dyna User's Conference, Dearborn, Michigan, 2006.

[7] R. Zemčík, V. Laš, T. Kroupa, H. Purš, Identification of material characteristics of sandwich panels, Bulletin of Applied Mechanics 26 (2011) 26-30.

[8] Abaqus 6.11 Documentation, Dassault Systèmes Simulia Corp., 2011.